

Sintering behaviour and mechanical properties of hydroxyapatite and dicalcium phosphate

PAUCHIU E. WANG, T. K. CHAKI

Department of Mechanical and Aerospace Engineering, State University of New York, Buffalo, NY 14260, USA

The sintering behaviour of powders of two calcium phosphates, namely hydroxyapatite (HA) and dicalcium phosphate (DCP), were studied at various temperatures and in various environments. The density, flexural strength and Knoop hardness of HA sintered in air for 4 h initially increased with the sintering temperature, reaching maxima at around 1150 °C, and then decreased due to decomposition of HA into tri- (TCP) and tetracalcium phosphates. Sintering in vacuum caused decomposition of HA at lower temperatures, and consequently the mechanical properties were poorer than those of HA sintered in air. The densification and mechanical properties of DCP sintered in air and vacuum showed similar behaviour to those of HA. In air DCP underwent phase transformation from γ - to β - and to α -phases. In vacuum DCP started to decompose into tricalcium phosphate at 1000 °C. To reduce dehydroxylation, HA powder was sintered in moisture at various temperatures up to 1350 °C and X-ray diffraction study did not indicate any decomposition at the highest sintering temperature. The density, flexural strength and hardness of HA sintered in moisture increased with the sintering temperature and eventually reached plateaux at about 1300 °C, but below 1200 °C they were lower than those of HA sintered in air at corresponding temperatures. Thus, it is seen that dehydroxylation did not hinder sintering of HA. On the other hand, decomposition obstructed sintering of both HA and DCP.

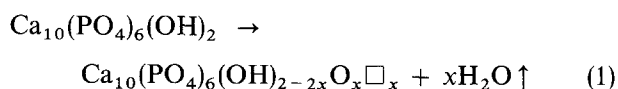
1. Introduction

Calcium phosphates [1] are major constituents of bone and hold great promise as biomaterials [2] for bone implantation, since they have the ability of bonding to bone [3]. The major phase [4] found in bone is HA [chemical formula $\text{Ca}_{10}(\text{PO}_4)_6(\text{OH})_2$]. Quite often, however, defective HA occurs with a Ca/P ratio deviated from $10/6 = 1.67$. Other commonly known phases are DCP, TCP and tetracalcium phosphate [chemical formulae $\text{Ca}_2\text{P}_2\text{O}_7$, $\text{Ca}_3(\text{PO}_4)_2$ and $\text{Ca}_4\text{P}_2\text{O}_9$, respectively].

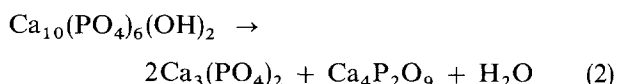
Blocks of HA with various densities and strengths can be prepared [5] by pressureless sintering, hot pressing and hot isostatic pressing. Winter *et al.* [6] suggested that there is a correspondence between the compactness of calcium phosphate implants and physiological acceptance. Studies of porous HA implants on the alveolar ridges of dogs [7] and human maxillary alveolus [8] demonstrated bone ingrowth into the open pores on the surface of the implants. Similar studies in dogs [9, 10] and biopsy specimens from humans [11, 12] showed that dense HA implants became surrounded by mature fibrous tissue, with a variable amount of new bone formation. However, HA implants often developed cracks [6, 10]. Thus, an optimization of the strength and microstructure of HA implants by a suitable choice of sintering parameters is needed. De Groot [13] indicated 1300 °C as the crit-

ical sintering temperature for calcium phosphates with Ca/P ratio between 1.5 and 1.7.

Sintering of HA is complicated by two processes, namely dehydroxylation and decomposition of HA at elevated temperatures. In dehydroxylation HA loses OH radicals upon heating [14] according to the equation



The hydroxyl ion-deficient product, $\text{Ca}_{10}(\text{PO}_4)_6(\text{OH})_{2-2x}\text{O}_x\Box_x$ (\Box = vacancy, $x < 1$) is known as oxyhydroxyapatite (OHA), whose existence has been identified [14, 15] by X-ray diffraction and infrared spectroscopic studies. In air OHA is formed at around 900 °C and in water-free environment it is formed at around 850 °C. Upon heating at higher temperatures, HA can decompose [16, 17] into TCP and tetracalcium phosphate according to



The objective of this study was to investigate how sintering of HA is affected by dehydroxylation and decomposition. We sintered HA in air, vacuum and moisture in the temperature range 900–1350 °C. For comparison we also sintered DCP, which does not

have any dehydroxylation problem owing to the absence of the OH radical in its molecule.

2. Materials and methods

The HA powder was synthesized by a wet-chemical method [18, 19]. Analytical grade $\text{Ca}(\text{NO}_3)_2 \cdot 4\text{H}_2\text{O}$ and $(\text{NH}_4)_2\text{HPO}_4$ were used as the starting materials: 286 cm³ aqueous solution of 0.3 M $(\text{NH}_4)_2\text{HPO}_4$ was poured into 400 cm³ 0.7 M $\text{Ca}(\text{NO}_3)_2$ aqueous solution. Immediately 30% NH_4OH solution (approximately 300 cm³) was added to the mixture and the pH was adjusted to 10.5. White precipitates were aged with stirring at 90 °C for 24 h. Precipitates were filtered, washed three times with distilled water and dried at 105 °C for 48 h. The dried product was ball-milled and calcined in air at 800 °C for 3 h. The calcined product was ball-milled again and the resultant powder was raw HA used for the sintering study. DCP powder of 99.95 wt % purity was purchased from Johnson Matthey Co. The particle sizes in the HA and DCP powders were examined with an optical microscope.

The Ca/P atomic ratio in raw HA was measured by chemical analysis. HA powder was dissolved in 50% concentrated HCl and the concentration of Ca ions in the solution was measured by atomic absorption spectrometry. The concentration of PO_4 ions was determined from the ultraviolet absorption spectrum of a molybdivanadophosphate complex [20]. Powders of HA and DCP were examined in a Nicolet X-ray diffractometer using CuK_α radiation. The diffraction patterns were compared with the database in the American Society for Testing and Materials powder diffraction files.

Powders of HA and DCP were compacted at room temperature inside steel dies under a uniaxial stress of 350 MPa. For lubrication the interior surfaces of the die were coated by applying a layer of stearic acid with a brush and then drying. The green compacts were prepared in rectangular shapes of two sizes, 14 mm × 7 mm × 6 mm and 48 mm × 7 mm × 5 mm. The green compacts of HA were sintered in air, vacuum and moisture for 4 h in the temperature range 900–1350 °C. The green compacts of DCP were sintered in air and vacuum for 4 h in the temperature range 850–1300 °C. The sintering in vacuum was done inside a water-cooled steel chamber with graphite heating elements. The chamber was flushed several times with argon and pumped by a mechanical pump. The pressure during sintering was about 27 Pa. The sintering in moisture was done by placing the samples in an alumina tube with the closed end inserted into a muffle furnace. The moisture was flowed through the tube at the rate of 0.07 m³ h⁻¹. After sintering, in all cases the specimens were cooled in the furnace, typically at a rate of 100 °C h⁻¹.

To determine the densification due to sintering, 14 mm long specimens were ground with emery papers to a precise rectangular shape (within 0.05 mm). To avoid absorption of water during density measurements, the grinding was done in the dry condition. The volume of the rectangular block was calculated from

the dimensions measured with the help of a slide caliper, and its weight was measured by a balance. The surface of some of the blocks was polished with alumina slurry up to 0.1 μm. The hardness was measured by Knoop indentation on the shiny surface. The load applied during Knoop indentation was 200 g. For metallographic examination a few rectangular blocks were cut in cross-section. The cross-sections were ground with emery paper and polished with alumina slurry up to 0.1 μm. To reveal the grain structure, the polished cross-sections were etched. A mixture in the ratio 1:1 of aqueous solutions of 85% concentrated lactic acid and 0.12 M ethyldiaminetetraacetic acid was applied for 10 s on the polished surface of HA. The etchant for DCP was prepared by dissolving 44 g $\text{K}_2\text{Cr}_2\text{O}_7$ into 1000 ml distilled water and mixing the solution with 2000 ml 48% concentrated HF, and was applied for 5 s. The polished cross-section was examined by optical microscopy.

The sintered bars (48 mm long) were used for measuring the flexural strength. Four-point bending tests were performed on the sintered bars following a US Military Standard [21]. The distance between the outer rollers was 40 mm. The fracture surfaces of the specimens broken by four-point bending were examined by scanning electron microscopy.

3. Results and discussion

3.1. X-ray diffraction

The powder X-ray diffraction pattern (Fig. 1a) of raw HA, calcined at 800 °C, did not contain any peak other

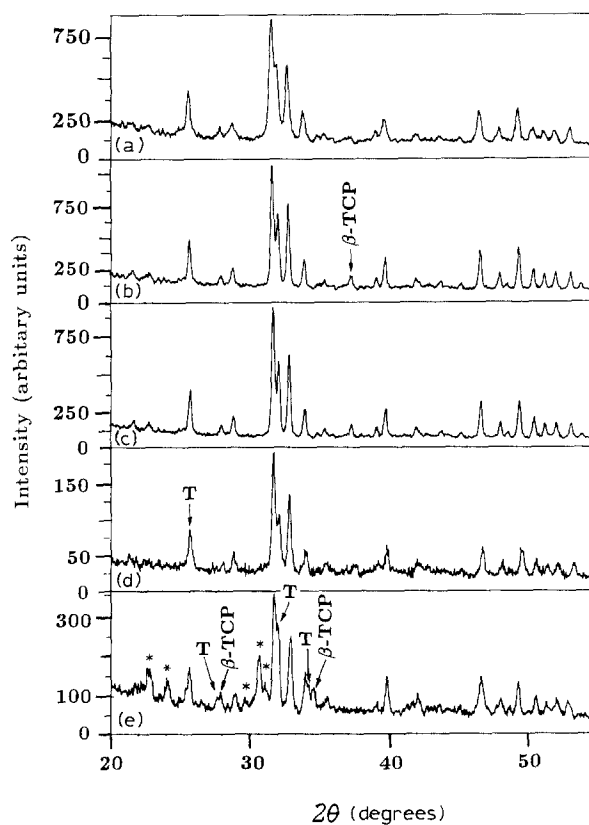


Figure 1 Powder X-ray diffraction patterns of HA sintered for 4 h in air at various temperatures: (a) raw HA, (b) 1100 °C, (c) 1200 °C, (d) 1300 °C and (e) 1350 °C. T, $\text{Ca}_4\text{P}_2\text{O}_9$; *, α -TCP.

than those of HA. It should be noted, however, that the presence of a small amount of amorphous calcium phosphate could not be detected by X-ray diffraction. However, it is expected that calcination at 800 °C had crystallized most of the amorphous phase. The Ca/P ratio in raw HA was measured as 1.69 ± 0.01 , which is very close to the Ca/P ratio (1.67) of perfect HA. Thus, it can be safely assumed that our starting HA powder (raw HA) was of good quality.

Fig. 1b–e shows the X-ray diffraction patterns of HA sintered for 4 h in air at 1100, 1200, 1300 and 1350 °C, respectively. During sintering at 1100 °C HA started to decompose and a peak due to β -TCP was observed (Fig. 1b). Upon sintering at 1300 °C peaks due to tetracalcium phosphate appeared (Fig. 1d). During sintering at 1350 °C some of the β -TCP was converted to α -TCP (Fig. 1e). Although decomposition of HA started during sintering in air at 1100 °C, dehydroxylation of HA in air occurred at lower temperatures. The X-ray diffraction peaks of HA sintered in air at 900 and 1000 °C for 4 h shifted by 0.1–0.2° of 2θ (Table I), indicating that the HA lattice had contracted due to loss of OH radicals. This behaviour of dehydroxylation is consistent with other reported works [14, 15]. When HA was sintered in moisture, no shift in the X-ray diffraction peaks was observed even after sintering at 1300 °C for 4 h. Thus, dehydroxylation of HA can be prevented by sintering in moisture. Furthermore, decomposition of HA was also prevented by sintering in moisture. Fig. 2a–d shows the powder X-ray diffraction patterns of HA sintered for 4 h in moisture at 1100, 1200, 1300 and 1350 °C, respectively and there was no sign of decomposition at the highest sintering temperature. Fig. 3a–d shows the powder X-ray diffraction patterns of HA sintered for 4 h in vacuum at 1000, 1100, 1200 and 1300 °C, respectively. At a sintering temperature as low as 1000 °C in vacuum there was clear peak of α -TCP formed by decomposition of HA. Thus, in vacuum, where dehydroxylation can take place at temperatures as low as 850 °C [14], the decomposition of HA can take place at temperatures lower than the decomposition temperature in air.

DCP can exist in three phases, namely α , β and γ [22]. Raw DCP in the as-received condition contained essentially γ -phase, as shown in the powder X-ray diffraction pattern of Fig. 4a. Fig. 4b–f shows the powder X-ray diffraction patterns of DCP sintered for 4 h in air at 900, 1000, 1100, 1200 and 1300 °C, respectively. Upon sintering in air at 900 °C DCP was transformed to β -phase. After sintering in air at 1300 °C DCP essentially consisted of α -phase, but no de-

TABLE I Positions of X-ray diffraction peaks of HA, showing dehydroxylation

(hkl)	2θ (degrees) after sintering at various temperatures		
	Raw	900 °C	1000 °C
(002)	25.73 ± 0.02	25.94	25.87
(211)	31.75 ± 0.01	31.87	31.85
(202)	34.01 ± 0.05	34.17	34.10

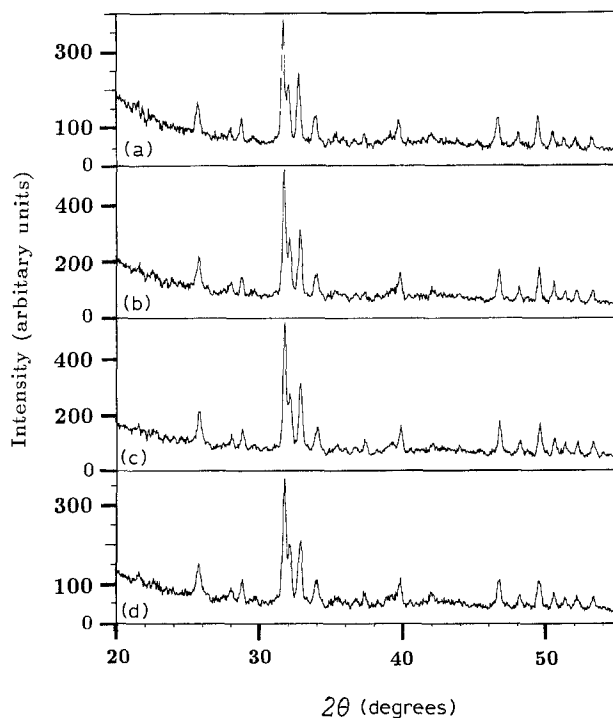


Figure 2 Powder X-ray diffraction patterns of HA sintered for 4 h in moisture at various temperatures: (a) 1100 °C, (b) 1200 °C, (c) 1300 °C and (d) 1350 °C.

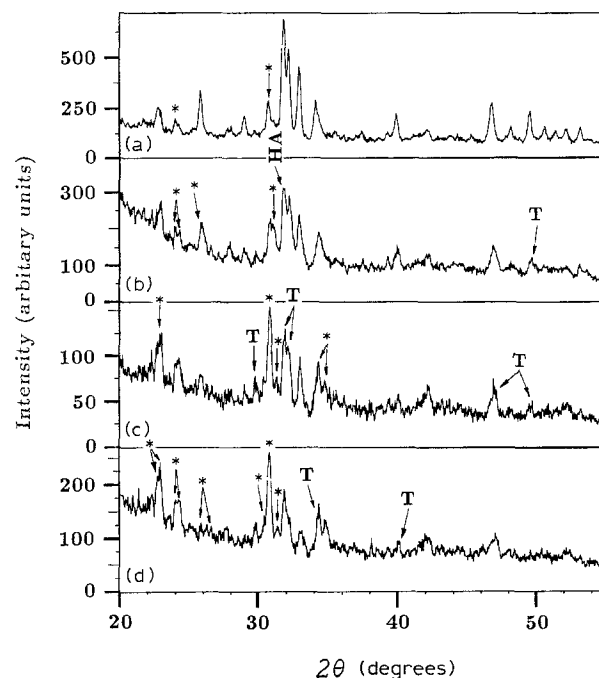


Figure 3 Powder X-ray diffraction patterns of HA sintered for 4 h in vacuum at various temperatures: (a) 1000 °C, (b) 1100 °C, (c) 1200 °C and (d) 1300 °C. T, $\text{Ca}_4\text{P}_2\text{O}_9$; *, α -TCP.

composition of DCP was observed, even though the sintering temperature was close to the melting point (1353 °C) of α -DCP [23]. Fig. 5a–e shows the powder X-ray diffraction patterns of DCP sintered for 4 h in vacuum at 900, 1000, 1100, 1200 and 1300 °C, respectively. In vacuum the decomposition of β -DCP to TCP started at the sintering temperature of 1000 °C. Upon sintering in vacuum at 1200 °C most of the DCP decomposed into a mixture of α - and β -TCP and

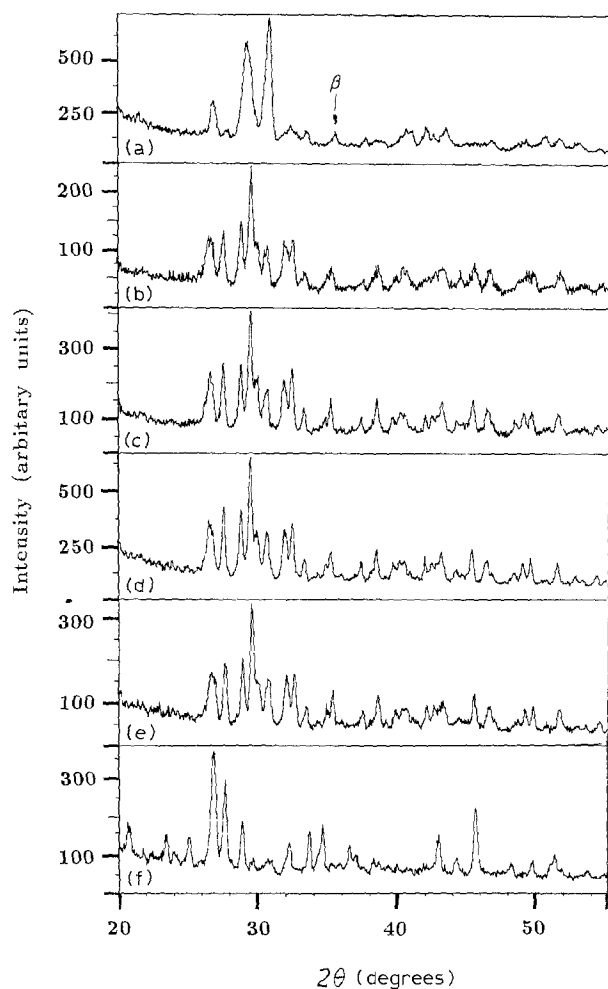


Figure 4 Powder X-ray diffraction patterns of DCP sintered for 4 h in air at various temperatures. (a) raw DCP. (b) 900 °C, (c) 1000 °C, (d) 1100 °C, (e) 1200 °C and (f) 1300 °C.

P₂O₅. It seems that vacuum acted as a reducing environment to cause the decomposition of DCP.

3.2. Densification and microstructure

Eighty per cent of the particles in the raw HA and DCP powders had sizes in the ranges 10–20 μm and 2–8 μm, respectively. The green densities of HA and DCP compacted by a uniaxial stress of 350 MPa were 1.96 ± 0.10 and 1.89 ± 0.15 g cm⁻³, respectively. Assuming that raw HA was composed of perfect HA of theoretical density 3.08 g cm⁻³, the green compacts of HA had a relative density of $64 \pm 3\%$. Since the raw DCP powder contained mostly γ-phase with a small amount of β-phase (both having a density of 3.00 g cm⁻³), the green compacts of DCP had relative density of $61 \pm 5\%$. It should be noted that α-DCP has a density of 2.93 g cm⁻³, which is lower than those of β- and γ-phases.

The densities of blocks sintered in various environments are given in Table II. The density of HA blocks sintered in air at 900 °C for 4 h was 1.89 ± 0.04 g cm⁻³, which is slightly lower than the green density. This decrease in density upon sintering at 900 °C in air was due to the loss of water by dehydroxylation of HA. However, the sinterability of OHA was good, as evidenced by the increase in density with

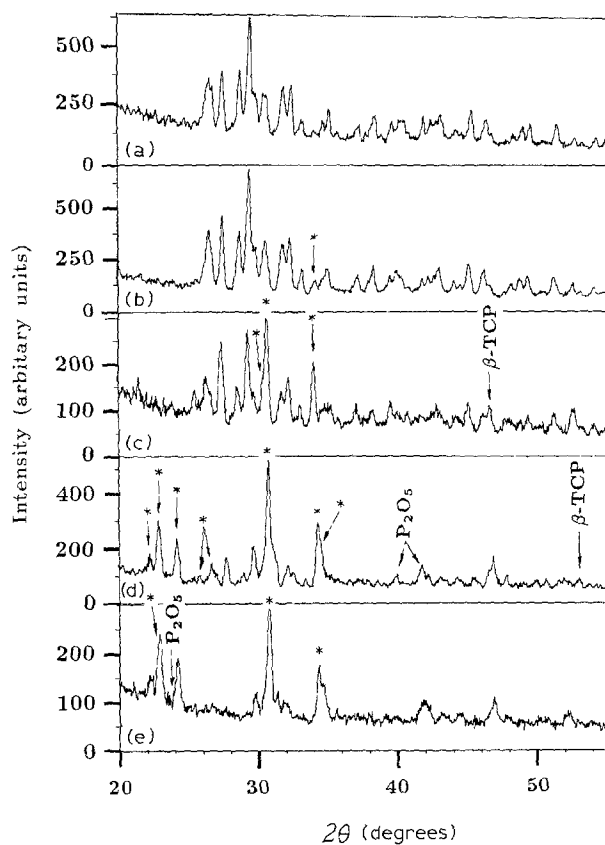


Figure 5 Powder X-ray diffraction patterns of DCP sintered for 4 h in vacuum at various temperatures (a) 900 °C, (b) 1000 °C, (c) 1100 °C, (d) 1200 °C and (e) 1300 °C. *, γ-TCP.

increasing sintering temperature. The density of HA blocks sintered in air at 1100 °C for 4 h was 2.46 ± 0.07 g cm⁻³. As seen in Fig. 6, the densification of HA was maximum at a sintering temperature of about 1150 °C in air. When the sintering temperature in air was > 1200 °C the density of the HA blocks decreased rapidly. The decrease in the density of sintered HA at high temperatures is attributed to decomposition which can obstruct sintering. As discussed in Section 3.1, the decomposition of HA in air started at 1100 °C.

Fig. 7 shows the microstructure of an HA specimen sintered in air at 1200 °C for 4 h. Due to brittleness, it was difficult to obtain a good polished surface of HA specimens. The mean intercept grain size, as measured from the optical micrograph (Fig. 7), was 90 μm and the average pore size was 20 ± 5 μm.

Densification of HA due to sintering for 4 h in vacuum follows (Fig. 6) a similar behaviour to those for sintering in air. However, the maximum density occurred at a lower sintering temperature (about 1050 °C), because in vacuum dehydroxylation and decomposition of HA can occur at temperatures lower than when sintering in air. At sintering temperatures < 1050 °C the densification of HA in vacuum was greater than that in air. For example, at the sintering temperature of 1000 °C the densities of blocks of HA sintered for 4 h in air and vacuum were 2.17 ± 0.03 and 2.36 ± 0.05 g cm⁻³, respectively. In vacuum, where dehydroxylation can take place at temperatures as low as 850 °C, OHA was formed rapidly at the beginning of the sintering cycle at 1000 °C and

TABLE II Density, Knoop hardness and flexural strength of HA sintered in air, in vacuum and in moisture for 4 h (values are means \pm standard deviation)

	Temperature ($^{\circ}\text{C}$)						
	900	1000	1100	1200	1250	1300	1350
Air							
Density (g cm^{-3})	1.89 ± 0.04	2.17 ± 0.03	2.46 ± 0.07	2.45 ± 0.12	2.07 ± 0.05	2.08 ± 0.10	2.03 ± 0.02
Hardness (MPa)	449 ± 11	850 ± 20	2035 ± 16	1771 ± 18	835 ± 19	647 ± 32	518 ± 15
Flexural strength (MPa)	3.8 ± 0.4	9.9 ± 0.8	14.0 ± 0.4	14.7 ± 0.2	7.4 ± 0.2	5.6 ± 0.9	4.6 ± 0.2
Vacuum							
Density (g cm^{-3})	1.91 ± 0.02	2.36 ± 0.05	2.39 ± 0.09	2.08 ± 0.04	1.98 ± 0.03	1.96 ± 0.08	1.93 ± 0.07
Hardness (MPa)	285 ± 30	627 ± 30	1630 ± 102	1292 ± 128	661 ± 25	488 ± 36	384 ± 148
Flexural strength (MPa)	3.8 ± 0.6	6.2 ± 0.5	11.6 ± 0.9	6.0 ± 0.8	4.3 ± 0.7	4.0 ± 0.2	4.0 ± 0.7
Moisture							
Density (g cm^{-3})	1.91 ± 0.05	1.96 ± 0.06	2.04 ± 0.07	2.18 ± 0.10	2.40 ± 0.03	2.43 ± 0.08	2.46 ± 0.07
Hardness (MPa)	155 ± 6	189 ± 2	298 ± 34	849 ± 30	928 ± 20	963 ± 34	1025 ± 16
Flexural strength (MPa)	3.6 ± 0.5	7.8 ± 0.4	10.5 ± 0.8	12.0 ± 0.3	15.3 ± 0.3	16.5 ± 0.4	16.4 ± 0.7

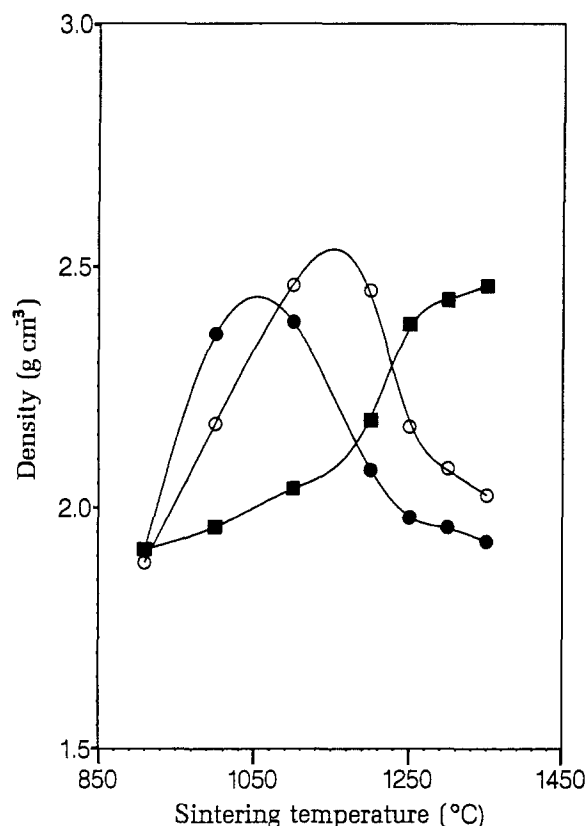


Figure 6 The densification of HA plotted against the sintering temperature in various environments (\circ) air, (\bullet) vacuum and (\blacksquare) moisture.

then OHA was densified by sintering. In contrast, upon sintering in moisture for 4 h at 1000°C the density of HA blocks was only $1.96 \pm 0.06 \text{ g cm}^{-3}$. In moisture, where no dehydroxylation was observed, the densification at 1000°C was lower than those in air and vacuum. Thus, comparing the densification at 1000°C in air, vacuum and moisture, it can be concluded that sinterability of OHA was better than that of HA.

The densification of HA in moisture increased monotonically (Fig. 6) with the sintering temperature, eventually reaching a plateau. As no decomposition of HA occurred in moisture at the highest sintering

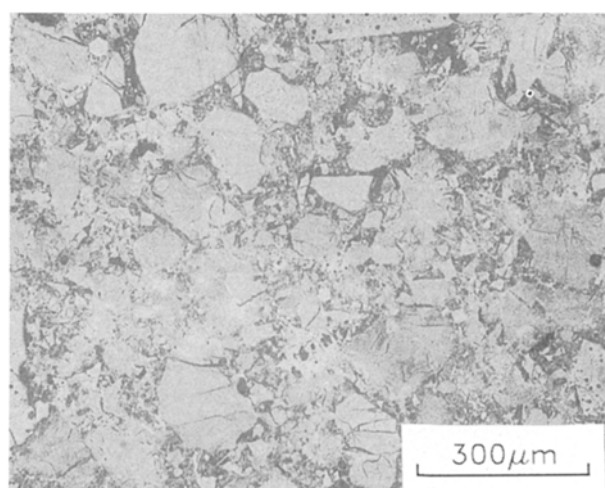


Figure 7 Optical micrograph of polished and etched surface of an HA specimen sintered in air at 1200°C for 4 h.

temperature of 1350°C , the densification in moisture did not show any decrease even at the highest sintering temperature. At and above the sintering temperature of 1250°C the densification in moisture was higher than the corresponding densifications in air and vacuum, where decomposition of HA was a serious problem above 1200°C . Thus, from the study of densification of HA due to sintering in air, vacuum and moisture, it can be concluded that decomposition and not dehydroxylation affected the sintering adversely.

Table III shows the densification of DCP in air and vacuum at various temperatures. Within the sintering temperature range $850\text{--}1300^{\circ}\text{C}$ the density versus sintering temperature curves (Fig. 8) were almost flat with a variation in density within 0.1 g cm^{-3} . Upon sintering in air for 4 h at 1000°C the density of DCP blocks reached a maximum value of $2.78 \pm 0.09 \text{ g cm}^{-3}$. At sintering temperatures above 1000°C in air the density decreased slightly. As discussed in Section 3.1, in air DCP did not decompose at the highest sintering temperature of 1300°C , but a transformation from β - to α -phase occurred. The

TABLE III Density, Knoop hardness and flexural strength of DCP sintered in air and in vacuum for 4 h (values are means \pm standard deviation)

	Temperature ($^{\circ}$ C)					
	850	900	1000	1100	1200	1300
Air						
Density (g cm^{-3})	2.73 ± 0.10	2.74 ± 0.14	2.78 ± 0.09	2.76 ± 0.10	2.74 ± 0.10	2.72 ± 0.15
Hardness (MPa)	3321 ± 17	3336 ± 18	3896 ± 15	3659 ± 16	3399 ± 16	3028 ± 22
Flexural strength (MPa)	29.4 ± 0.8	31.2 ± 1.0	32.3 ± 0.9	28.4 ± 0.9	26.3 ± 1.0	26.0 ± 0.4
Vacuum						
Density (g cm^{-3})	2.44 ± 0.07	2.47 ± 0.05	2.54 ± 0.03	2.49 ± 0.02	2.46 ± 0.04	2.45 ± 0.12
Hardness (MPa)	1241 ± 9	1383 ± 9	1811 ± 47	1600 ± 25	1301 ± 46	1274 ± 17
Flexural strength (MPa)	28.6 ± 0.1	30.0 ± 0.3	30.5 ± 0.7	26.5 ± 0.4	26.4 ± 0.9	25.9 ± 1.1

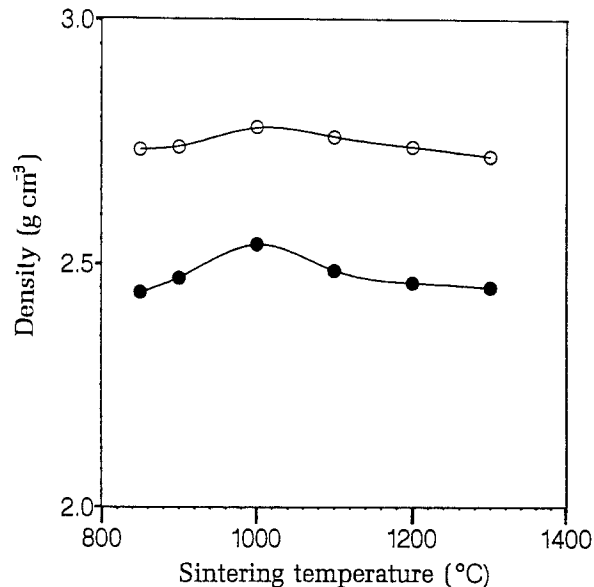


Figure 8 The densification of DCP plotted against the sintering temperature in different environments: (○) air and (●) vacuum.

transformation from β - to α -phase of DCP is accompanied by a volume increase that can produce an internal pressure to obstruct sintering. Fig. 9 shows the microstructure of a DCP specimen sintered in air for 4 h at 1000° C. The mean intercept grain size of the specimen was $75 \mu\text{m}$ and the average pore size was $10 \pm 3 \mu\text{m}$.

The sintering behaviour of DCP in vacuum was similar to that in air. However, the densities of DCP blocks sintered in vacuum were lower (Fig. 8) than the corresponding densities obtained by sintering in air. The density of DCP blocks reached a maximum value of $2.54 \pm 0.03 \text{ g cm}^{-3}$ upon sintering in vacuum for 4 h at 1000° C. When sintered in vacuum at temperatures above 1000° C the density of DCP blocks decreased. As discussed in Section 3.1, DCP decomposed due to sintering in vacuum at temperatures above 900° C. The decomposition of DCP affected the sintering in vacuum adversely and, consequently, the densification in vacuum was lower than that in air at corresponding temperatures.

3.3. Knoop hardness

The Knoop hardness (measured under 200 g load) of HA blocks sintered in various environments for 4 h is

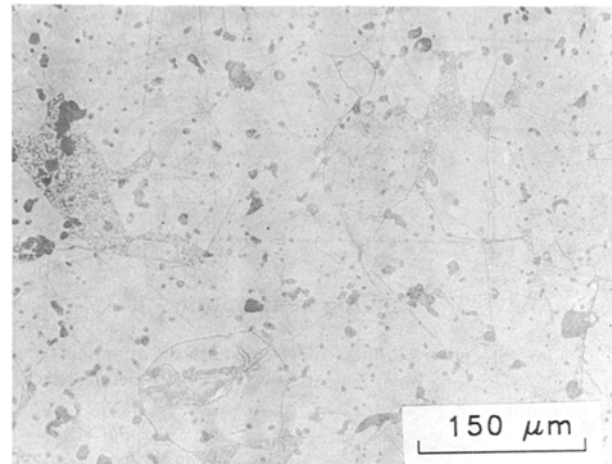


Figure 9 Optical micrograph of polished and etched surface of a DCP specimen sintered in air at 1000° C for 4 h.

given in Table II. The variation in the hardness of HA with sintering temperature (Fig. 10) was similar to that of densification, indicating that hardness was controlled by the bonding among the particles in the sintered compacts. The hardness of HA blocks sintered both in air and in vacuum increased rapidly with the sintering temperature, reaching the maximum value at about 1150° C, and then decreased at higher sintering temperatures. The hardness of HA blocks sintered in vacuum was always lower than that of HA sintered in air at corresponding temperatures. The hardnesses of HA blocks sintered in air and vacuum for 4 h at 1100° C were 2035 ± 16 and $1630 \pm 102 \text{ MPa}$, respectively. Decomposition of HA in vacuum at relatively low sintering temperatures obstructed the development of bonding between the particles in the sintered compacts and was responsible for lower hardness obtained upon vacuum-sintering compared with that obtained upon air-sintering. However, the hardness of HA sintered in moisture for 4 h at 1100° C was only $298 \pm 34 \text{ MPa}$, due to the poor sinterability of hydroxylated HA. The hardness of HA compacted in moisture increased monotonically with the sintering temperature, eventually reaching a plateau.

The Knoop hardness values of DCP blocks sintered for 4 h in air and in vacuum at various temperatures are shown in Table III. Fig. 11 shows how the Knoop hardness of DCP compacts changed with the sintering

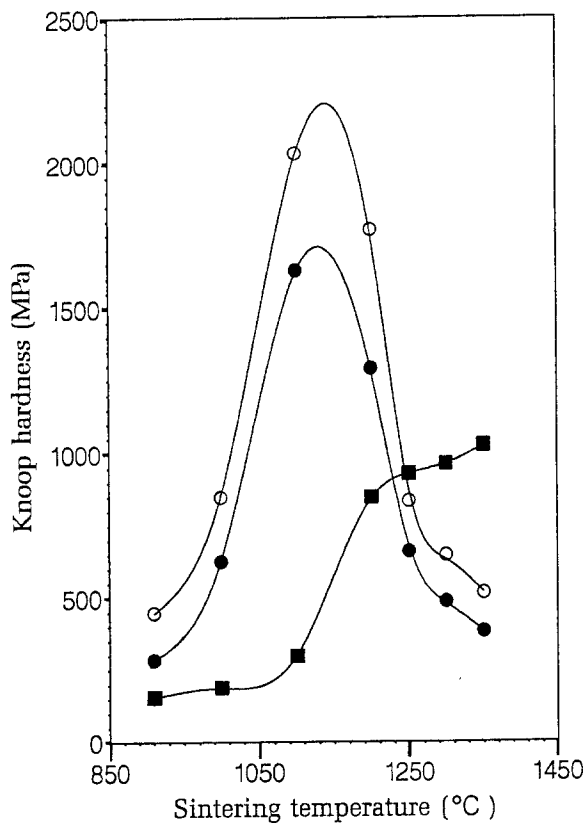


Figure 10 Knoop hardness of HA against the sintering temperature in various environments: (○) air, (●) vacuum and (■) moisture

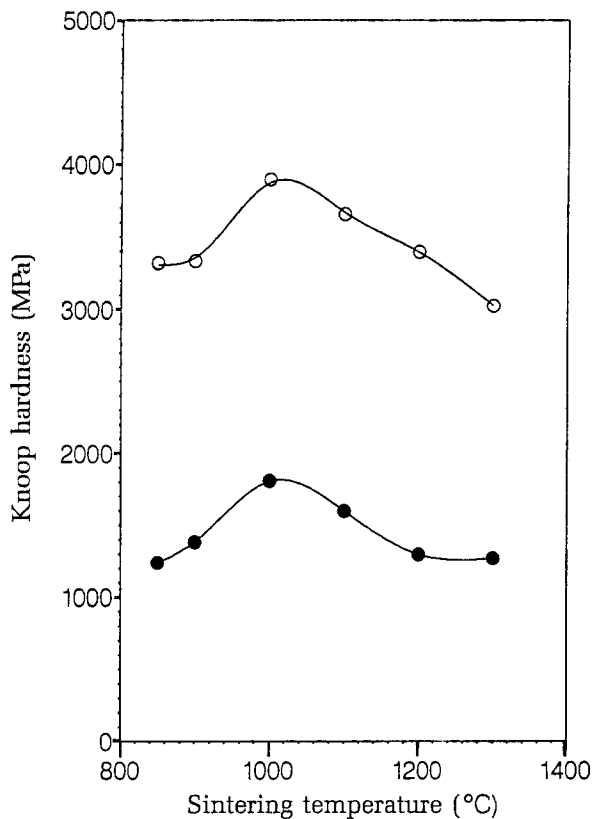


Figure 11 Knoop hardness of DCP plotted against the sintering temperature in different environments: (○) air and (●) vacuum

temperature. The variation in hardness of DCP with sintering temperature was similar to the variation in the densification. The hardness values of DCP sin-

tered both in air and in vacuum initially increased with the sintering temperature, reaching maximum values at about 1000 °C, and then started to decrease. As discussed in earlier sections, the phase transformation in DCP obstructed sintering in air and, consequently, the Knoop hardness decreased upon sintering at temperatures above 1000 °C. In vacuum the decomposition of DCP caused a decrease in the hardness at sintering temperatures above 1000 °C. In fact, the decomposition hindered sintering so badly that the hardness values of DCP sintered in vacuum were much lower than those obtained by sintering in air at the corresponding temperatures. The Knoop hardness of DCP compacts sintered in vacuum for 4 h at 1000 °C was 1811 ± 47 MPa, compared with 3896 ± 15 MPa obtained upon sintering in air for 4 h at 1000 °C.

3.4. Flexural strength

The flexural strengths of HA compacts sintered in air, vacuum and moisture for 4 h at various temperatures are given in Table II. The variation in the flexural strength of HA with sintering temperature (Fig. 12) followed a behaviour similar to that of the densification. The flexural strengths of HA bars sintered in air and vacuum initially increased with sintering temperature, reaching the maximum values at about 1150 and 1100 °C, respectively, and then decreased at higher sintering temperatures. Due to the decomposition of HA in vacuum at relatively low temperatures, the flexural strength of HA sintered in vacuum was

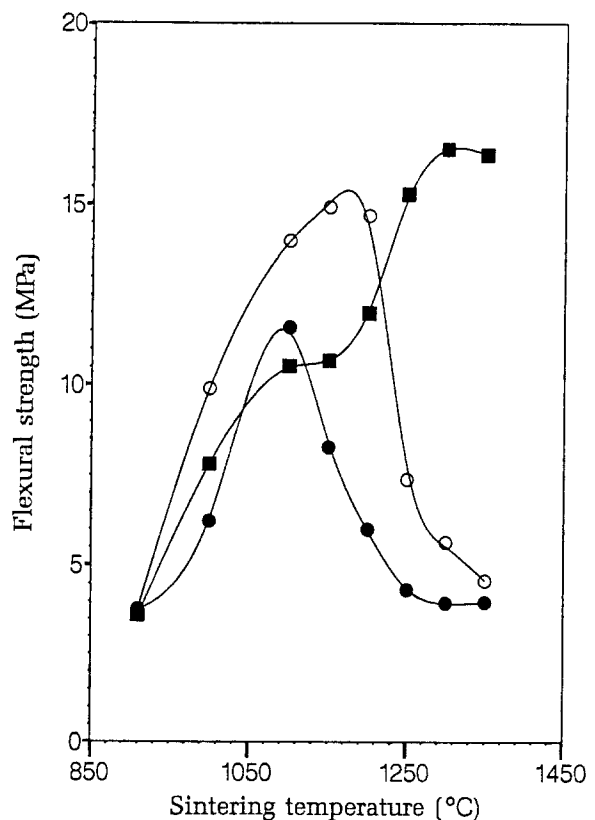


Figure 12 Flexural strength of HA plotted against the sintering temperature in various environments: (○) air, (●) vacuum and (■) moisture.

always lower than that of HA sintered in air at corresponding temperatures. The flexural strengths of HA bars sintered in air and vacuum for 4 h at 1100 °C were 14.0 ± 0.4 and 11.6 ± 0.9 MPa, respectively. The flexural strength of HA sintered in moisture for 4 h at 1100 °C was 10.5 ± 0.8 MPa, being lower than those obtained upon sintering in air and in vacuum at 1100 °C. However, the flexural strength of HA sintered in moisture increased with the sintering temperature, reaching a steady value of 16.5 MPa at 1300 °C.

The flexural strengths of DCP bars sintered for 4 h in air and in vacuum at various temperatures are shown in Table III. The strengths increased with the sintering temperature (Fig. 13), reaching the maximum values at about 1000 °C, and then decreased. Below the sintering temperature of 1200 °C the flexural strengths of DCP sintered in vacuum were lower than those obtained upon sintering in air. The flexural strengths of DCP bars sintered in air and in vacuum for 4 h at 1000 °C were 32.3 ± 0.9 and 30.5 ± 0.7 MPa, respectively. These values are almost twice the maximum flexural strength (16.5 MPa) of HA bars obtained upon sintering in moisture for 4 h at 1300 °C. A similar comparison can be made for the hardness values of sintered HA and DCP. Such comparisons indicate that the mechanical properties of sintered DCP are superior to those of sintered HA. Even in the hydroxylated state, the sinterability of HA is poorer than that of DCP.

An examination of the fracture surfaces (Fig. 14) produced by flexural tests revealed interesting information concerning the nature of fracture. The HA bar sintered in air for 4 h at 1200 °C showed intergranular fracture (Fig. 14a), whereas HA sintered in moisture for 4 h at 1300 °C failed predominantly by cleavage (Fig. 14b). In both cases some particles of HA powder, possibly due to poor sintering, were seen on the fracture surfaces. The DCP bar sintered in air for

4 h at 1000 °C failed by cleavage mode (Fig. 14c) and the fracture surface was clean. It should be noted that high-density ceramics typically fail by cleavage at room temperature.

The HA bars sintered in air for 4 h at 1200 °C and sintered in moisture for 4 h at 1300 °C had almost identical densities and flexural strengths (Table II).

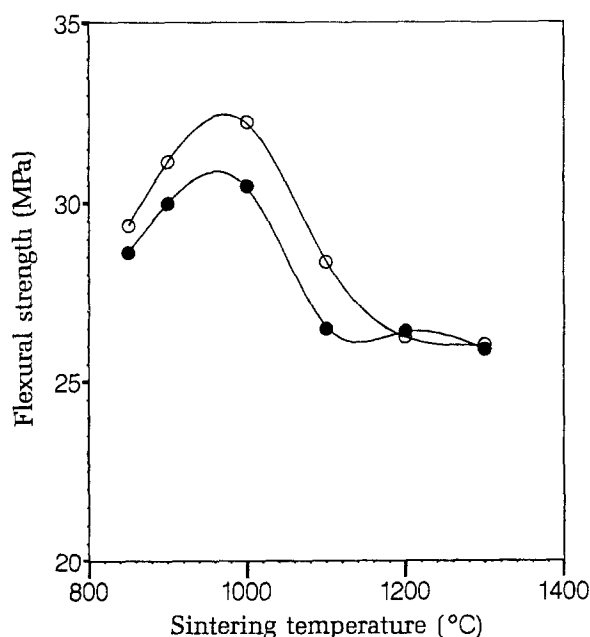


Figure 13 Flexural strength of DCP plotted against the sintering temperature in different environments: (○) air and (●) vacuum.

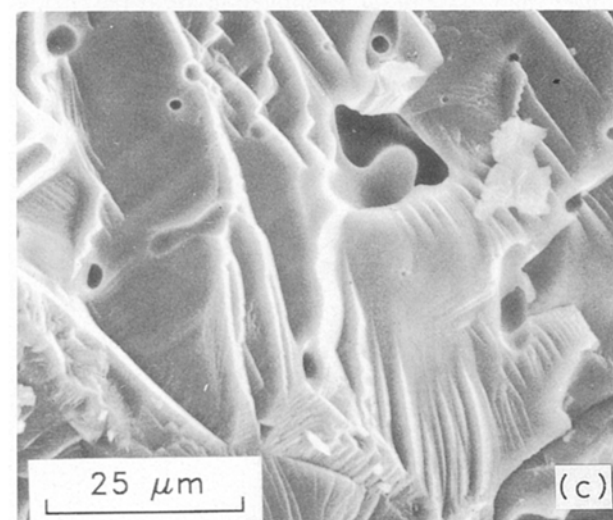
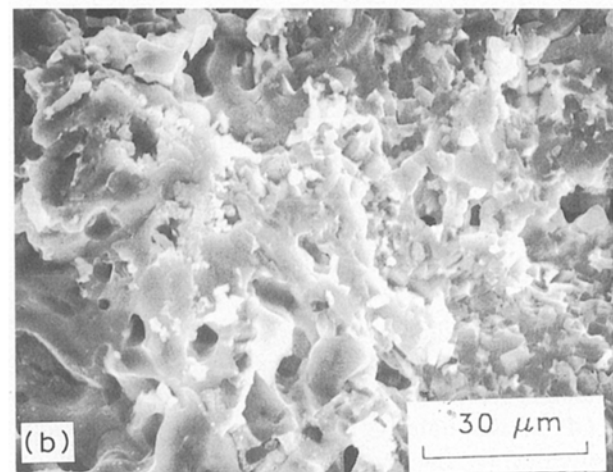
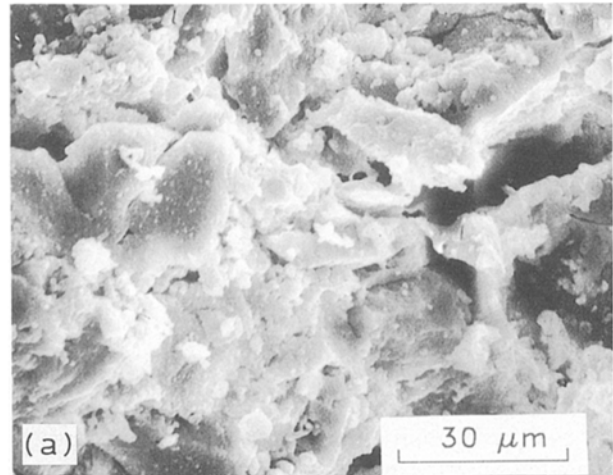


Figure 14 Scanning electron micrographs of fracture surfaces: (a) HA sintered in air for 4 h at 1200 °C, (b) HA sintered in moisture for 4 h at 1300 °C and (c) DCP sintered in air for 4 h at 1000 °C

However, HA sintered in air had weaker grain boundaries than HA sintered in moisture, and hence failed by intergranular fracture. A possible cause of weak grain boundaries in HA sintered in air may be the presence of decomposition products at grain boundaries. In fact, the presence of decomposition products at grain boundaries of HA sintered in air at 1250 °C for 1 h was reported by Jarcho *et al.* [19]. Even though the grain boundaries of HA sintered in moisture are strong, the almost identical flexural strengths of HA sintered in moisture at 1300 °C and HA sintered in air at 1200 °C only indicate the inherent brittle nature of hydroxylated HA.

4. Conclusion

HA powder was sintered in air, in vacuum and in moisture in the temperature range 900–1350 °C. DCP powder was sintered in air and in vacuum in the temperature range 850–1300 °C. Dehydroxylation of HA in air and vacuum took place in the temperature range 850–900 °C, but did not obstruct sintering, as evidenced by an increase in densification with sintering temperature. However, decomposition of HA in air and in vacuum at higher sintering temperatures hindered sintering and caused decreases in the density, flexural strength and Knoop hardness of HA compacts sintered at temperatures above 1150 °C. In moisture, however, HA did not show any indication of dehydroxylation or decomposition, even at the highest sintering temperature of 1350 °C. However, below the sintering temperature of 1200 °C the density, flexural strength and hardness of HA compacts sintered in moisture were lower than those of HA sintered in air at the corresponding temperatures, indicating that the sinterability of hydroxylated HA is poorer than that of OHA.

In air DCP did not decompose, but its sinterability was limited by structural phase transformation. In vacuum, however, DCP started to decompose into TCP at the sintering temperature of 1000 °C and, consequently, the density, flexural strength and hardness of DCP compacts sintered in vacuum were much lower than those of DCP sintered in air at the corresponding sintering temperatures. The maximum flexural strength of DCP was 32.3 ± 0.9 MPa, obtained upon sintering in air for 4 h at 1000 °C, and was about twice that of HA bars sintered in moisture for 4 h at 1300 °C, indicating that the sinterability of DCP is better than that of HA.

Acknowledgements

Partial support from the University at Buffalo Bio-

medical Research Support Grant through the National Institutes of Health, USA, is acknowledged. We also thank Professor George Nancollas of State University of New York at Buffalo for his kind help in the measurement of the Ca/P ratio in HA.

References

1. J R VAN WAZER, "Phosphorous and Its Compounds", Vols I and II (Interscience, New York, 1958).
2. J S HANKER and B L GIAMMARA, *Science* **242** (1988) 885.
3. M. JARCHO, *Clin. Orthopaed. Related Res.* **157** (1981) 259.
4. C. LAVERNIA and J. M. SCHOENUNG, *Ceram. Bull.* **70** (1991) 95.
5. H DENISSEN, C MANGANO and G VENINI, "Hydroxylapatite Implants" (Piccin Nuova Libreria, SPA, Padua, 1985) p. 19.
6. M. WINTER, P. GRISS, K. DE GROOT, H TAGAI, G HEIMKE, H J A V. DIJK and K SAWAI, *Biomaterials* **2** (1981) 159.
7. R E. HOLMES and S. M. ROSER, *Int. J. Oral Maxillofac. Surg.* **16** (1987) 718.
8. J. W. FRAME, P. G. J. ROUT and R. M. BROWNE, *ibid.* **18** (1989) 142.
9. C. CHANG, V. J. MATUKAS and J. E. LEMONS, *ibid.* **41** (1983) 729.
10. G. L. DE LANGE, C. DE PUTTER, K. DE GROOT and E. H. BURGER, *J. Dent. Res.* **68** (1989) 509.
11. S.-Y. CHAO and C.-K. POON, *J. Oral Maxillofac. Surg.* **45** (1987) 359.
12. D. G. PAGE and D. LASKIN, *ibid.* **45** (1987) 356.
13. K. DE GROOT, *Biomaterials* **1** (1980) 47.
14. J. C. TROMBE and G. MONTEL, *J. Inorg. Nucl. Chem.* **40** (1978) 15.
15. T. KIJIMA and M. TSUTSUMI, *J. Amer. Ceram. Soc.* **62** (1979) 455.
16. W. VAN RAEMDONCK, P. DUCHEYNE and P. DE MEESTER, in "Metal and Ceramic Biomaterials", Vol. 2, edited by P. Ducheyne and W. Hasting (CRC Press, Boca Raton, Florida, 1984) p. 149.
17. H. NEWESELY, *J. Oral Rehab.* **4** (1977) 97.
18. K. YAMASHITA, H. OWADA, H. NAKAGAWA, T. UMEGAKI and T. KANAZAWA, *J. Amer. Ceram. Soc.* **69** (1986) 590.
19. M. JARCHO, C. H. BOLEN, M. B. THOMAS, J. BOBICK, J. F. KAY and R. H. DOREMUS, *J. Mater. Sci.* **11** (1976) 2027.
20. A. GEE and V. R. DEITZ, *Analyt. Chem.* **25** (1953) 1320.
21. Military Standard MIL-STD-1942 (MR), "Flexural Strength of High Performance Ceramics at Ambient Temperature" (Department of the Army, Washington, DC, 1983).
22. P. W. RANBY, D. H. MASH and S. T. HENDERSON, *Brit. J. Appl. Phys.* **8** (1957) S18.
23. W. L. HILL, G. T. FAUST and D. S. REYNOLDS, *Amer. J. Sci.* **242** (1944) 457.

Received 8 May

and accepted 20 July 1992